Supplementary Table S1. The correlation between ALDH1A3 protein expression and percentage of $ALDH^+$ cells in NSCLC lines (Data for Figure 2D).

Cell Line	% $ALDH^+$ Cells	ALDH1A3 Protein Expression[a]	ALDH1A1 Protein Expression[a]
H1819	38	54	0
H661	28	57	298
H358	17	119	0
HCC193	16	58	NA
H2087	14	109	0
A549	7	1	628
H1395	6	22	NA
H2009	4	3	0
H441	4	26	NA
H1155	3	4	0
H1993	2	4	0
HCC1195	2	0.4	NA
H2073	1	7	0
H2887	1	2	NA
H157	1	4	NA
H460	1	1	0
H650	0.4	0.2	NA
H23	0.1	2	NA
H2085	0	27	NA
H2126	0	6	NA

[a]ALDH1A3 or ALDH1A1 relative western blot band densitometry intensity normalized to GAPDH x100.

Correlation between %$ALDH^+$ cells and ALDH1A3 protein expression is $r = 0.67$.

0 = no band detected on western blots

NA (not available)

Supplementary Table S2. Incidence of xenograft tumors derived from control or ALDH1A3 knockdown lung cancer cells.

NSCLC Cells Tested	**Cells Injected**			***P* value**
	10^5	**10^4**	**10^3**	
	(# tumors/# mice)			
H358-shGFP	5/5	5/5	3/5	
H358-shALDH1A3	5/5	5/5	1/5	
H2087-shGFP	5/5	4/5	3/5	<0.0001
H2087-shALDH1A3	3/5	0/5	0/5	

Probability of a difference between control and shALDH1A3 group was determined by Chi-square test.

Supplementary Table S3. The association between ALDH1A3 protein expression and clinicopathological variables for 455 NSCLC patient samples

Variables	No. (%)	$ALDH1A3^{high}$ ≥150	$ALDH1A3^{low}$ <150	*P* value
Gender				
Male	225 (49.5)	105 (46.7)	120 (53.3)	**0.018**
Female	230 (50.5)	134 (58.3)	96 (41.7)	
Histological Type				
AD	295 (64.8)	198 (67.1)	97 (32.9)	**0.0001**
SCC	160 (35.2)	41 (25.6)	119 (74.4)	
Smoking Status				
Never	50 (11)	38 (76)	12 (24)	**0.0005**
Former	215 (47.3)	115 (53.5)	100 (46.5)	
Current	190 (41.7)	86 (45.3)	104 (73.7)	
Disease Stage				
Stage I	236 (51.9)	131 (55.5)	105 (44.5)	0.27
Stage II	109 (24)	52 (47.7)	57 (52.3)	
Stage III	97 (21.3)	47 (48.6)	50 (51.5)	
Stage IV	13 (2.8)	9 (69.2)	4 (30.8)	
Node Involvement				
N0	306 (67.3)	164 (53.6)	142 (46.4)	0.68
N1	79 (17.4)	38 (48.1)	41 (51.9)	
N2	70 (15.4)	37 (52.9)	33 (47.1)	
Disease Stage				
T1	160 (35.2)	86 (53.8)	74 (46.2)	0.74
T2	236 (51.9)	126 (53.4)	110 (46.6)	
T3	26 (5.7)	12 (46.2)	14 (53.8)	
T4	33 (7.2)	15 (45.4)	18 (54.6)	
Differentiation				
Status				

Well	50 (11)	39 (78)	11 (22)	**0.0001**
Moderately	236 (51.9)	126 (53.4)	110 (46.6)	
Poorly	169 (37.1)	74 (43.8)	95 (56.2)	

Chi-square test.

Supplementary Figure Legends

Figure S1. ALDH profiling of 8 NSCLC lines using the flow cytometry based Aldefluor assay.

Figure S2. Anchorage dependent colony formation efficiency was determined by growing serial dilutions of sorted $ALDH^+$ and $ALDH^-$ cells for 2 weeks in liquid culture.

Figure S3. A, ALDH1A3 protein expression in a set of NSCLC lines was detected by western blots. The corresponding percentage of $ALDH^+$ cells was analyzed by Aldefluor assay. B, western blot showed ALDH1A1 protein expression in certain HBEC and NSCLC lines. C, ALDH1A3 was knocked down using three siRNAs in a panel of NSCLC lines with different driver mutations followed by liquid colony formation assays. RT-PCR was performed to examine ALDH1A3 mRNA expression. The plot revealed that depletion of ALDH1A3 reduced the ability of most NSCLC cells to form liquid colonies *in vitro* except for H3122 cells. D, Knocking down ALDH1A3 in sorted ALDH+ H358 cells using siRNAs significantly reduced both ALDH1A3 mRNA expression and liquid colony forming ability.

Figure S4. Ectopic expression of ALDH1A3 does not affect tumorigenicity of lung cancer cells. A, overexpression of ALDH1A3 in H2009 cells was detected by western blot. B, the percentage of $ALDH^+$ cells was significantly increased by ectopic expression of ALDH1A3 in H2009 cells. C, overexpressed ALDH1A3 did not enhance anchorage dependent colony forming ability in H2009 cells. D, limiting dilutions of H2009-pCMV and H2009-pCMV-ALDH1A3 cells were injected subcutaneously into NOD/SCID mice and tumor growth was monitored for 8 weeks.

Supplementary Fig. S1

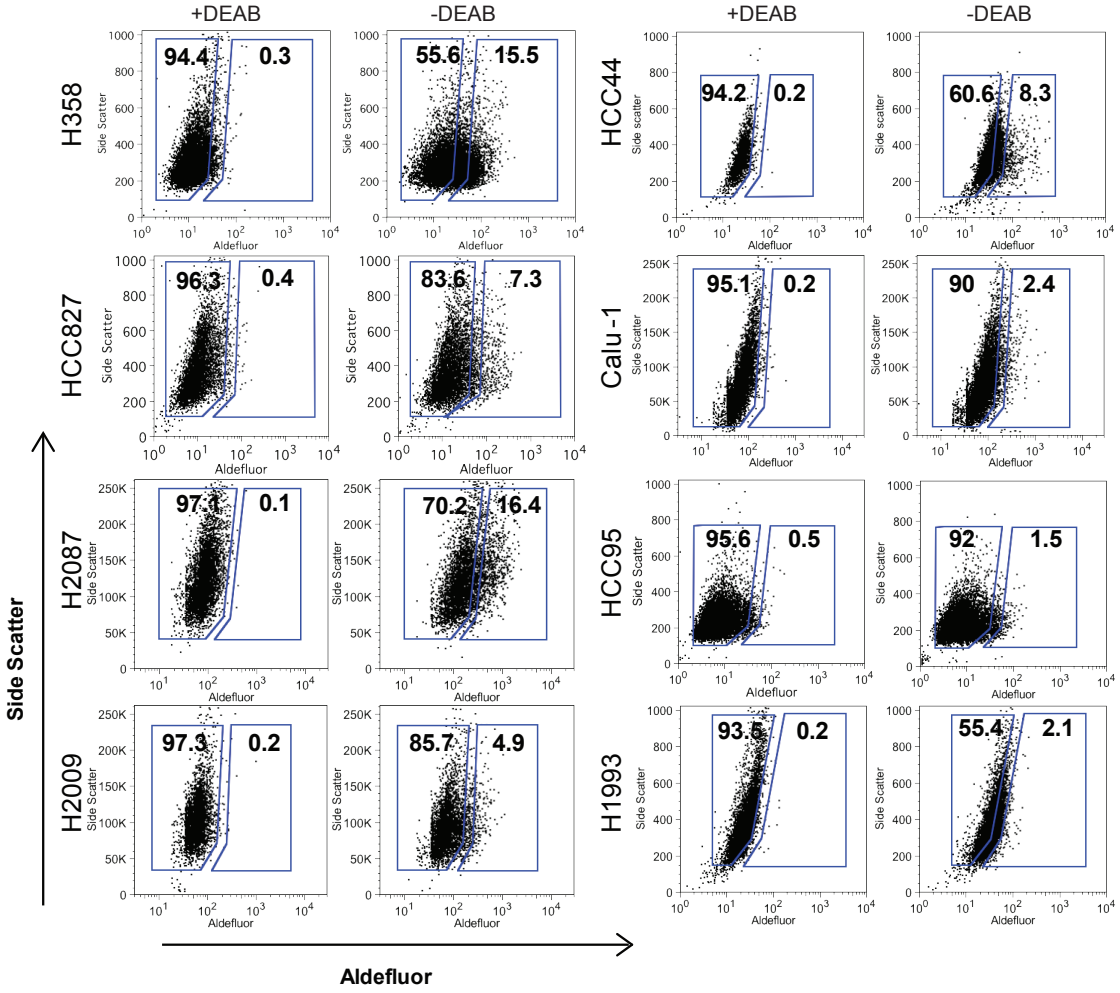

Supplementary Fig. S2

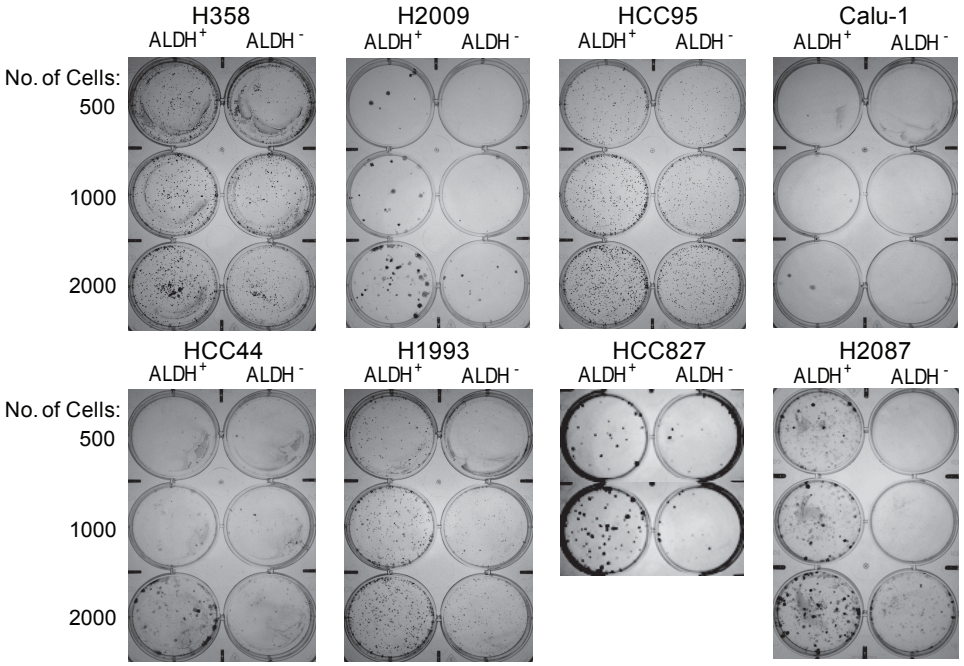

Supplementary Fig. S3

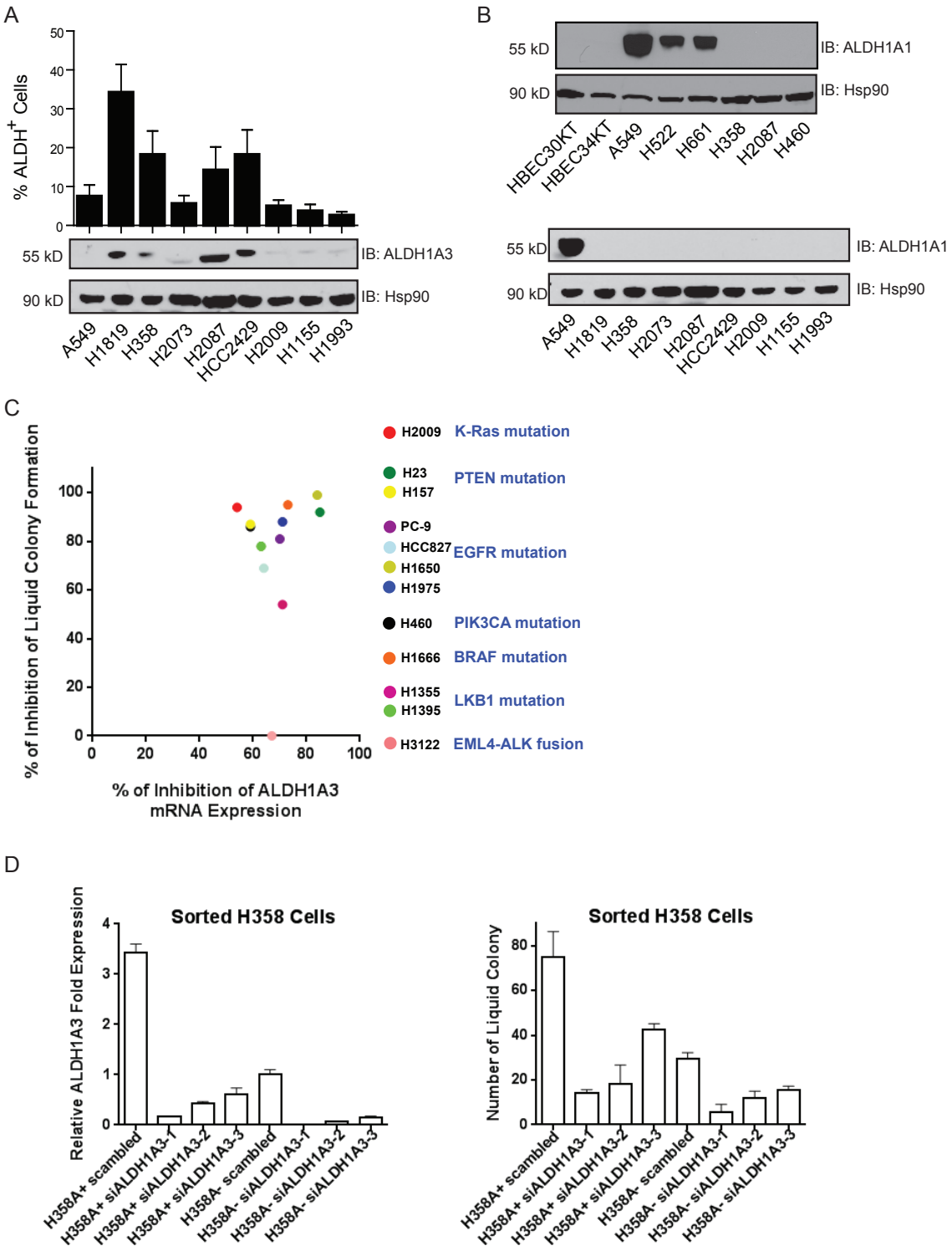

Supplementary Fig. S4